

Published in final edited form as:

*Am J Obstet Gynecol.* 2015 February ; 212(2): 174.e1–174.e7. doi:10.1016/j.ajog.2014.08.008.

## Impact Of Prolapse Meshes On The Metabolism Of Vaginal Extracellular Matrix In Rhesus Macaque

Rui Liang, MD<sup>1</sup>, Wenjun Zong, MD, PhD<sup>1</sup>, Stacy Palcsey, BS<sup>1</sup>, Steve Abramowitch, PhD<sup>2</sup>, and Pamela A. Moalli, MD, PhD<sup>1</sup>

<sup>1</sup>Magee Women Research Institute, Department of Obstetrics and Gynecology, School of Medicine, University of Pittsburgh

<sup>2</sup>Department of Bioengineering, Swanson School of Engineering, University of Pittsburgh

### Abstract

**Objective**—The impact of polypropylene mesh implantation on vaginal collagen and elastin metabolism was analyzed using a nonhuman primate model to further delineate the mechanism of mesh induced complications.

**Methods**—49 middle aged parous rhesus macaques underwent surgical implantation of 3 synthetic meshes via sacrocolpopexy. Gynemesh PS (n=12) and two lower weight, higher porosity, lower stiffness meshes - UltraPro (n = 19) and Restorelle (n=8) were implanted, in which UltraPro was implanted with its blue orientation lines perpendicular (low stiffness direction, n=11) and parallel (high stiffness direction, n=8) to the longitudinal axis of vagina. Sham operated animals were used as controls (n=10). Twelve weeks after surgery, the meshtissue complex was excised and analyzed.

**Results**—Relative to Sham, Gynemesh PS had a negative impact on the metabolism of both collagen and elastin favoring catabolic reactions while UltraPro only induced an increase in elastin degradation. Restorelle had the least impact. As compared to Sham, the degradation of collagen and elastin in the vagina implanted with Gynemesh PS was increased with a simultaneous increase in active MMP-1, -8, -13 and total MMP-2, -9 (all P<0.05). The degradation of elastin (tropoelastin and mature elastin) was increased in the UltraPro implanted vagina with a concomitant increase of MMP-2, and -9 (all P<0.05). Collagen subtype ratio III/I was increased in both Gynemesh PS and UltraPro perpendicular groups (P<0.05).

© 2014 Elsevier Inc. All rights reserved.

Corresponding author: Pamela A. Moalli, Magee Women Research Institute, Department of Obstetrics and Gynecology, 204 Craft Ave., Pittsburgh, PA 15219, Phone: +1-412-641-6012, Fax: +1-412-641-5290, moalpa@mail.magee.edu.

The authors report no conflict of interest.

Some findings were presented at the 33rd Annual Meeting of the American Urogynecology Society, Chicago, Illinois, October 2012.

**Condensation:** The heavier, less porous and stiffer mesh Gynemesh PS increased the catabolism of collagen and elastin in the vagina, characterized by increased matrix degradation and MMPs.

**Publisher's Disclaimer:** This is a PDF file of an unedited manuscript that has been accepted for publication. As a service to our customers we are providing this early version of the manuscript. The manuscript will undergo copyediting, typesetting, and review of the resulting proof before it is published in its final citable form. Please note that during the production process errors may be discovered which could affect the content, and all legal disclaimers that apply to the journal pertain.

**Conclusion**—Following implantation with the heavier, less porous and stiffer mesh, Gynemesh PS, the degradation of vaginal collagen and elastin exceeded synthesis, most likely as a result of increased activity of MMPs, resulting in a structurally compromised tissue.

### Keywords

Synthetic mesh; vagina; collagen and elastin; MMPs; rhesus macaque

---

### Introduction

Lightweight polypropylene mesh has been widely used in the surgical repair of pelvic organ prolapse to improve anatomical outcomes<sup>1-2</sup>. However, mesh related complications including mesh exposure through the vaginal wall and erosion into adjacent structures, pain and infection, have raised concerns, prompting the FDA to issue two public health notifications warning of complications related to prolapse mesh and calling for mechanistic studies<sup>3-5</sup>.

To date, the impact of mesh on the vagina has not yet been clearly defined, and the mechanism by which mesh complications occur remains unknown. In a well-controlled nonhuman primate sacrocolpopexy model, heavier weight, low porosity and higher stiffness meshes were shown to have a profoundly negative impact on the vagina including a decrease in the amount of collagen, elastin and smooth muscle<sup>6</sup>. The resulting thinner and biomechanically inferior vagina seemed a perfect scenario for the development of mesh exposure, a process in which mesh becomes visible through the vaginal epithelium. Since collagen and elastin are key structural proteins that maintain the mechanical and structural integrity of vagina, their content and stability are likely critical factors in the pathogenesis of mesh exposures.

In this study, we aimed to define alterations in collagen and elastin metabolism following the implantation of synthetic meshes varying by weight, porosity and stiffness. We hypothesized that heavier, less porous and stiffer meshes would be associated with increased collagen and elastin degradation characterized by increased matrix metalloproteinases (MMPs) and an increased ratio of collagen subtypes III/I. To test this hypothesis, we compared the impact of three distinct polypropylene meshes with varying textile and structural properties - the heavier, lower porosity and stiffer prolapse mesh (Gynemesh PS, Ethicon, Sommersville, NJ) vs. two lighter, higher porosity and lower stiffness meshes *with* (Ultrapro, Ethicon, Sommersville, NJ) and *without* (Restorelle, Coloplast, Minneapolis, MN) an absorbable component - poliglecaprone 25. Meshes were implanted via sacrocolpopexy in the Rhesus Macaque. Since UltraPro is highly anisotropic<sup>7-8</sup>, it was implanted with its blue orientation lines perpendicular (low stiffness direction) and parallel (high stiffness direction) to the longitudinal axis of the vagina. The production and degradation of collagen and elastin, collagen subtype III/I ratio as well as the levels of matrix metalloproteinases (MMP) MMPs -1, -2, -8, -9 and -13 were examined.

## Materials and Methods

### Mesh

Sterile samples of Gynemesh PS, UltraPro and Restorelle were obtained. Their structural properties were defined using an established tensile testing protocol<sup>6,9</sup>.

### Animals

Animal groups in the current study were the same as those in a previous study<sup>6</sup> except that a new animal was added to the UltraPro Perpendicular group. Parous middle aged non-human primates (Rhesus Macaques) were maintained and treated according to protocols approved by the Institutional Animal Care Use Committee of the University of Pittsburgh (IACUC #1008675) and in adherence to the National Institutes of Health Guidelines for the use of laboratory animals.

### Surgical procedures

Two animals were excluded from the study at the time of surgery – the first due to a large mass in her right leg and enlarged pelvic lymph nodes, and a second with stage IV endometriosis. In the end, a total of 49 animals were used. Thirty nine animals were implanted with mesh via sacrocolpopexy after hysterectomy<sup>6</sup>: Gynemesh PS (n=12), UltraPro Perpendicular (n=11), UltraPro Parallel (n=8), and Restorelle (n=8). Ten animals underwent the identical surgery (Sham) without insertion of mesh (n=10). Twelve weeks later, the mesh-tissue complex was harvested *en toto* and the epithelium was carefully removed prior to biochemical analyses.

### Western Blot – precursors of collagen I, and III

Following extraction using a high salt buffer (pH 7.5), total protein concentration was determined in duplicate (DC Protein Assay, Bio-Rad Laboratories, Hercules, CA). Proteins at 10µg/well were separated on 8% polyacrylamide gels and examined by standard procedures on a Western Blot. Precision plus Protein<sup>TM</sup> WesternC<sup>TM</sup> Standards (Bio-Rad) were used to indicate the molecular weight. Primary antibodies included COL1A1 1:400 (L-19, goat polyclonal, Santa Cruz Biotechnology Inc., Santa Cruz, CA), and COL3A1 1:200 (C-15, goat polyclonal, Santa Cruz). Signal intensity of bands was quantitated via UN-SCAN-IT (version 4.3; Silk Scientific Co, Orem, UT). The blotted membranes were stained with Coomassie Blue and the protein bands were quantified to represent loading control for each well. Protein amounts were expressed as arbitrary units, relative to the loading control and an internal positive control (protein extracts from a human prolapsed vagina) that was loaded in duplicate on each gel.

### Western Blot – tropoelastin and tropoelastin degradation

Tropoelastin monoclonal 1:200 (BA-4, mouse, Abcam, Cambridge, MA) and polyclonal 1:400 (ab21605, rabbit, Abcam, Cambridge, MA) were used to detect tropoelastin ~60kD (monoclonal) and tropoelastin degradation products (series of bands less than 50kD) respectively. To reduce the amount of nonspecific binding by the polyclonal antibody, we: 1) established optimal binding conditions utilizing a progressive series of dilutions of the

primary antibody; and 2) confirmed the absence of nonspecific binding by the secondary antibody by performing parallel blots in which the primary antibody was eliminated.

### **Western Blot - matrix metalloproteinases MMPs -1, -8, and -13**

The primary antibodies including MMP-1 1:200 (41-1ES, mouse monoclonal, recognizing both latent and active forms; EMD Biosciences Inc, San Diego, CA), MMP-8 1:400 (115-13D2, mouse monoclonal, recognizing both latent and active forms, EMD), and MMP-13 1:200 (VIII A2, mouse monoclonal recognizing both proenzyme and active forms, EMD) were used. The band detection and quantification were similar to the procedures described above.

### **Gelatin zymography for MMPs -2, and -9**

The level of elastin degrading enzymes, MMPs-2 and -9, was evaluated via substrate zymography by using 30 µg protein per sample as described<sup>10</sup>.

### **Interrupted SDS-PAGE for collagen subtypes**

After protein extraction, the salt insoluble tissue pellets were used to determine the ratio of collagen subtypes III/I<sup>11,12</sup>. Following pepsin digestion, samples were isolated on 6% gels by interrupted sodium-dodecyl sulfate gel electrophoresis (SDS-PAGE). Purified collagen type I and III (Abcam, Cambridge, MA) and protein standards (pre-stained SDS-PAGE Standards High Range, Bio-Rad) were also run on the gels to indicate molecular weight. Semi-quantification of collagen bands was performed by densitometric scanning of protein bands corresponding to  $\alpha 1(I)$  and  $\alpha 1(III)$  chains on an imaging densitometer (Bio-Rad Laboratories, Hercules, CA). The relative collagen subtype III/I ratio was determined as  $\alpha 1(III) \times 2 / \alpha 1(I) \times 3$ .

### **Assay for degradation products of collagen - NTx**

Peptides less than 30kD were isolated using Centrifugal Filter Units (Amicon Ultra, 30,000MWCO, Millipore, MA). Total amounts of cross-linked N-telopeptides (NTx) including those derived from completely degraded collagen (end products) and those from intermediate collagen degradation fragments were measured using a standard NTx assay (Osteomark NTx, Princeton, NJ). The values were calculated using a 4-parameter standard curve and expressed as nmol/g protein normalized to collagen content. The samples were first digested with bacterial collagenase (Type I, 2mg/ml, Worthington, Lakewood, NJ) to degrade the intermediate collagen fragments prior to assaying for the total NTx. The amount of intermediate degradation products was estimated by subtracting the amount of NTx in the end products from total NTx.

### **Assays for degradation products of mature elastin**

The amount of desmosine, a crosslink that is characteristic of mature elastin, was measured in the less than 30kD peptide solution via a desmosine crosslink radioimmunoassay (crosslinks / total protein) as previously described<sup>13</sup>.

## Statistical analysis

SPSS software (14.0 student version for windows, Inc. SPSS) was used for statistical analyses. For normally distributed data, a one-way analysis of variance (ANOVA) was used followed by the appropriate post-hoc tests including Dunnett's for comparison to Sham and pairwise test using Bonferroni multiple comparisons procedure between all groups. For nonparametric data, a Kruskal-Wallis test was used.

## Results

Animals had similar age, parity, weight and POP-Q scores except that animals in the Restorelle group were heavier (Table 1).

### Synthesis of precursors of collagen and elastin

Two bands at ~140kD and ~200kD were detected representing the precursors of collagen I  $\alpha$ 1 (Figure 1A). The lower bands (~140kD) likely represent soluble collagen I  $\alpha$ 1 chains prior to cross-linking and incorporation into mature collagen fibrils. Collagen I precursors were significantly increased in all mesh groups relative to Sham, with an increase of 66%, 63%, 46% and 43% in Gynemesh PS ( $P=0.014$ ), UltraPro Perpendicular ( $P=0.023$ ), UltraPro Parallel ( $P=0.026$ ), and Restorelle ( $P=0.018$ ), respectively. No difference was found between the two UltraPro groups ( $P=0.57$ ). For precursors of collagen type III, a single band representing collagen III  $\alpha$ 1 chains was detected at ~160kD. As shown in Figure 1B, collagen III precursors increased 26% with Gynemesh PS ( $P=0.03$ ) and 29% with UltraPro Perpendicular ( $P=0.005$ ) while no differences were found relative to Sham in other mesh groups (all  $P>0.05$ ). Collagen III precursors were 45% higher in the UltraPro Perpendicular than the UltraPro Parallel group ( $P=0.004$ ). Bands for tropoelastin were detected at ~60kD (Figure 1C) with no significant differences found between the mesh groups and Sham (all  $P>0.05$ ).

### Collagen subtype III/I ratio in salt insoluble collagen

As shown in Figure 2, relative to Sham ( $0.20 \pm 0.05$ ), the ratio of collagen subtype III/I was 66% higher in Gynemesh PS ( $0.33 \pm 0.04$ ,  $P<0.001$ ) and 55% higher in UltraPro Perpendicular ( $0.31 \pm 0.06$ ,  $P<0.001$ ). No statistical difference was found in UltraPro Parallel ( $0.24 \pm 0.06$ ,  $P=0.08$ ) and Restorelle ( $0.25 \pm 0.09$ ,  $P=0.17$ ) relative to Sham. Comparison between the two UltraPro groups showed that the ratio was 26% higher in the perpendicular orientation than that in the parallel orientation ( $P=0.03$ ).

### Collagen degradation

NTx, a marker of mature collagen degradation, was assayed for both end products and intermediate products as a measurement of total collagen breakdown. As shown in Figure 3, consistent with our previous finding demonstrating a decrease in total mature collagen<sup>6</sup>, collagen degradation was increased by 62% in the Gynemesh PS group relative to Sham ( $P=0.007$ ). The other mesh groups were not statistically different from Sham (all  $P>0.05$ ). In addition, the intermediate collagen degradation products were increased by 89% in Gynemesh PS group ( $P=0.008$ ) relative to Sham while no significant increase was found in

the other groups. Collagen degradation was not different between the two UltraPro groups ( $P=0.513$  and  $P=0.909$ ).

### Elastin degradation

Previously, we showed that mature elastin was decreased following implantation with Gynemesh PS and UltraPro, independent of the direction of implantation but did not change with Restorelle<sup>6</sup>. To determine whether elastin degradation was accounting for these results, we measured both tropoelastin degradation and mature elastin degradation (Figure 4A). Mature elastin degradation products are identifiable by their desmosine crosslinks. Tropoelastin degradation was increased in all mesh groups relative to Sham, with the highest degradation in the Gynemesh PS group (119%,  $P=0.007$ ), followed by UltraPro Parallel (93%,  $P=0.015$ ), Restorelle (77%,  $P=0.042$ ), and UltraPro Perpendicular (71%,  $P=0.009$ ) (Figure 4B, 4C). Mature elastin degradation was increased in Gynemesh PS, UltraPro Perpendicular and UltraPro Parallel relative to Sham by an average increase of 76% ( $P=0.049$ ), 136% ( $P=0.006$ ) and 98% ( $P=0.025$ ), respectively, but not in the Restorelle group ( $P=0.589$ ) (Figure 4D). Elastin degradation in both tropoelastin and mature elastin pathways was not different between the UltraPro Perpendicular and Parallel groups ( $P=0.615$  and  $P=0.343$ ).

### Level of active MMPs

Active MMPs-1, -8 and -13 were significantly increased in the Gynemesh PS group compared to Sham with MMP-1 increased by 70% ( $P=0.014$ ), MMP-8 by 66% ( $P=0.048$ ), and MMP-13 by 71% ( $P=0.011$ ). In contrast, the amount of these MMPs was not different from Sham in the lighter, more porous UltraPro and Restorelle (all  $P>0.05$ , Figure 5A). Furthermore, no difference was found between the two UltraPro groups (all  $P>0.05$ ).

MMPs -2 and -9 were analyzed by substrate zymography (Figure 5B). As the bands between pro and active forms of MMP-9 were not always clearly separable, we analyzed them as a single band. For equipose, we analyzed MMP-2 similarly. Therefore, “total MMP-2” and “total MMP-9” are reported. When compared to Sham, total MMP-2 increased considerably following the implantation of Gynemesh PS, UltraPro Perpendicular and UltraPro Parallel by 114% ( $P=0.003$ ), 141% ( $P=0.046$ ) and 116% ( $P=0.045$ ) respectively, but not with Restorelle ( $P=0.11$ ). In addition, when compared to Sham, total MMP-9 increased in Gynemesh PS, UltraPro Perpendicular and UltraPro Parallel by 796% ( $P=0.007$ ), 925% ( $P=0.003$ ), and 719% ( $P=0.028$ ), respectively, but not Restorelle ( $P=0.109$ ). No difference was found between the two UltraPro groups (all  $P>0.05$ ).

### Comment

Following implantation with Gynemesh PS by sacrocolpopexy, the quantity of collagen and elastin in the grafted vagina decreased by 20% and 43%, respectively, with impaired tissue function as measured in biomechanical tests<sup>6,9</sup>. Here, we demonstrate that the decreases in these key structural proteins is via accelerated degradation associated with an increase in active MMPs including the interstitial collagenases MMPs-1, -8, and -13 and the elastases MMPs-2, and -9. While, at first glance our finding that implantation with Gynemesh PS



stimulates an increase in collagen I and III precursors, seems to contradict a degenerative process, we believe that the data reflect a highly active remodeling environment that persists 3 months after mesh implantation. Thus, even though synthesis of collagen precursors is taking place, degradation of these precursors and the mature products likely exceeds synthesis resulting in a net catabolic effect. Similar to our previous studies, in the current study, the heavier, lower porosity and higher stiffness mesh, Gynemesh PS, was associated with increased matrix degradation while meshes of lower weight, higher porosity and lower stiffness had less of a negative impact.

Elastin is a key protein in pelvic organ support<sup>14</sup>. A decrease in vaginal mature elastin content occurred following implantation with Gynemesh PS and UltraPro (regardless of direction) but not Restorelle<sup>6</sup>. The decrease, in the most part, was mirrored by increased degradation as measured by increased mature elastin degradation products and increased total MMP-2 and MMP-9. The absence of a change in the amount of tropoelastin and the increase in tropoelastin degradation that occurred in all of the groups suggests that tropoelastin is being degraded at a similar rate that it is synthesized, resulting in minimal net changes. For Gynemesh PS and UltraPro, the inability of tropoelastin to replenish the mature elastin which is being degraded by MMPs -2 and -9 resulted in a net loss.

Polypropylene behaves as foreign body when implanted into humans, inciting a classic foreign body response. During this process, inflammatory cells are recruited to the mesh insertion site where MMPs are secreted by these cells and resident cells to facilitate cell infiltration, adhesion and fusion, as well as the activation of proinflammatory cytokines<sup>15</sup>. Although necessary for the body to incorporate foreign materials, excessive and prolonged release/activation of MMPs can lead to the destruction of key matrix proteins, such as collagen and elastin, in the grafted and adjacent areas resulting in a deterioration of tissues structural and mechanical integrity<sup>15, 16</sup>. In the present study, the levels of activated MMPs-1, -2, -8, -9 and -13 increased after the implantation of Gynemesh PS, which correlate well with our previous observation that Gynemesh PS induced stronger foreign body inflammatory responses than meshes of lower weight, higher porosity and lower stiffness<sup>17, 18</sup>. As it is well established that the inflammatory reaction becomes stronger in proportion to the amount of material implanted<sup>16, 19, 20</sup>, the findings suggest that an increased mesh burden is more likely to induce prolonged activation of MMPs and excessive matrix destruction.

Mesh stiffness is a second critical parameter that impacts tissue responses by conferring inappropriate mechanical loading to the vagina. Indeed, the stiffness of a mesh has been previously purported to directly influence the occurrence of mesh exposure<sup>21-23</sup>. The stiffness of mesh determined in *ex vivo* testing may dramatically change following implantation, tensioning and loading. For example, Gynemesh PS undergoes a complete loss of porosity and an increase of stiffness at strains of just 4.9 N/cm, demonstrating the instability of mesh properties in response to even small loads<sup>24, 25</sup>. When the stiffness of implanted material is high, stressshielding of the underlying and associated tissues may increase the activity of MMPs resulting in tissue degeneration and a loss of mechanical integrity<sup>26-29</sup>. Our finding that higher stiffness Gynemesh PS induced the highest levels of MMPs is in line with this phenomenon.

The ratio of collagen subtype III/I was increased in the Gynemesh PS and UltraPro Perpendicular implanted vagina, but not with implantation of UltraPro Parallel and Restorelle. Such an increase could be the result of increased production of collagen III precursors in the former two groups. It is well known that an increase in the ratio of collagen subtype III/I is present in the default healing process and following microtrauma. Normally, the production of collagen type III peaks during the inflammatory phase of healing and decreases steadily thereafter<sup>30, 31</sup>. The persistent elevated ratio of collagen type III to I in the vagina three months after the implantation of Gynemesh PS and UltraPro Perpendicular indicates the presence of prolonged stimuli, possibly from chronic tissue injury caused by a gradual deformation/micromotion of mesh fibers under the loading conditions.

Indeed, in contrast to UltraPro Perpendicular in which the extremely wide pores (4mm) collapse under loading conditions simulating a sacrocolpopexy, the pore geometry of UltraPro Parallel is preserved, even though the mesh is stiffer when loaded uniaxially in this orientation. Similarly, the pores of Restorelle do not collapse when loaded in a sacrocolpopexy model<sup>25</sup>. Thus, the less negative impact of UltraPro parallel and Restorelle on the vagina highly suggests that the stability of pore geometry with loading is an important factor to consider. It is likely that, meshes in which pore geometry is preserved with loading afford increased tissue in-growth translating into improved outcomes.

The primary limitation of the study is that we were able to analyze only a limited number of meshes due to ethical considerations, for which we reduced the number of animals in the study to the lowest possible. However, we were able to define important differences in the impact of commonly used polypropylene meshes with different textile properties on the metabolism of key structural proteins in the vagina.

In summary, implantation with the heavier, less porous and stiffer mesh Gynemesh PS by sacrocolpopexy was associated with increased catabolism of collagen and elastin in the vagina, characterized by increased matrix degradation associated with an increase in MMPs. Lighter, more porous and less stiff meshes had less of negative impact. Future studies will define the mechanisms by which multiple MMPs are activated in response to different mesh properties.

## Acknowledgments

NIH funding support R01 HD061811-01. Assistance of **Dr. Barry Starcher** from University of Texas Health Science Center at Tyler, Department of Biochemistry, in examining total mature elastin content.

Study conducted at Pittsburgh, PA 15213, USA

Financial support provided by the National Institutes of Health (NIH) R01 HD061811-01

## References

1. Iglesia CB, Fenner DE, Brubaker L. The use of mesh in gynecologic surgery. *Int Urogynecol J Pelvic Floor Dysfunct.* 1997; 8:105–15. [PubMed: 9297599]
2. Jonsson Funk M, Edenfield AL, Pate V, Visco AG, Weidner AC, Wu JM. Trends in use of surgical mesh for pelvic organ prolapse. *Am J Obstet Gynecol.* 2013; 208:79 e1–7. [PubMed: 23159692]



3. Committee Opinion no. 513: vaginal placement of synthetic mesh for pelvic organ prolapse. *Obstet Gynecol.* 2011; 118:1459–64. [PubMed: 22105294]
4. Maher C, Feiner B, Baessler K, Schmid C. Surgical management of pelvic organ prolapse in women. *Cochrane Database Syst Rev.* 2013; 4:CD004014. [PubMed: 23633316]
5. Nygaard I, Brubaker L, Zyczynski HM, et al. Long-term outcomes following abdominal sacrocolpopexy for pelvic organ prolapse. *JAMA.* 2013; 309:2016–24. [PubMed: 23677313]
6. Liang R, Abramowitch S, Knight K, et al. Vaginal degeneration following implantation of synthetic mesh with increased stiffness. *BJOG.* 2013; 120:233–43. [PubMed: 23240802]
7. Feola A, Barone W, Moalli P, Abramowitch S. Characterizing the ex vivo textile and structural properties of synthetic prolapse mesh products. *Int Urogynecol J.* 2013; 24:559–64. [PubMed: 22885725]
8. Ozog Y, Konstantinovic M, Werbrouck E, De Ridder D, Mazza E, Deprest J. Persistence of polypropylene mesh anisotropy after implantation: an experimental study. *BJOG.* 2011; 118:1180–5. [PubMed: 21668770]
9. Feola A, Abramowitch S, Jallah Z, et al. Deterioration in biomechanical properties of the vagina following implantation of a high-stiffness prolapse mesh. *BJOG.* 2013; 120:224–32. [PubMed: 23240801]
10. Moalli PA, Shand SH, Zyczynski HM, Gordy SC, Meyn LA. Remodeling of vaginal connective tissue in patients with prolapse. *Obstet Gynecol.* 2005; 106:953–63. [PubMed: 16260512]
11. Niyibizi C, Kavalkovich K, Yamaji T, Woo SL. Type V collagen is increased during rabbit medial collateral ligament healing. *Knee Surg Sports Traumatol Arthrosc.* 2000; 8:281–5. [PubMed: 11061296]
12. Sykes B, Puddle B, Francis M, Smith R. The estimation of two collagens from human dermis by interrupted gel electrophoresis. *Biochem Biophys Res Commun.* 1976; 72:1472–80. [PubMed: 793589]
13. Starcher B, Conrad M. A role for neutrophil elastase in the progression of solar elastosis. *Connect Tissue Res.* 1995; 31:133–40. [PubMed: 15612329]
14. Drewes PG, Yanagisawa H, Starcher B, Hornstra I, Csiszar K, Marinis SI, Keller P, Word RA. Pelvic organ prolapse in fibulin-5 knockout mice: pregnancy-induced changes in elastic fiber homeostasis in mouse vagina. *Am J Pathol.* 2007; 170:578–89. [PubMed: 17255326]
15. Jones JA, McNally AK, Chang DT, et al. Matrix metalloproteinases and their inhibitors in the foreign body reaction on biomaterials. *J Biomed Mater Res A.* 2008; 84:158–66. [PubMed: 17607751]
16. Klinge U, Junge K, Stumpf M, AP AP, Klosterhalfen B. Functional and morphological evaluation of a low-weight, monofilament polypropylene mesh for hernia repair. *J Biomed Mater Res.* 2002; 63:129–36. [PubMed: 11870645]
17. Mani D, Nolfi A, Brown BN, Palcsey S, Moalli P. Chronic foreign body response following implantation of prolapse meshes in the rhesus macaque. *Female Pelvic Med Reconstr Surg.* 2013; 19(suppl 2):S89.
18. Klein-Patel M, Feola A, Stein S, Moalli PA. Ultra-lightweight synthetic mesh has similar cellular response but increased tissue ingrowth relative to heavier weight prototype. *Female Pelvic Med Reconstr Surg.* 2011; 17(suppl 1):S56.
19. Rosch R, Junge K, Schachtrupp A, Klinge U, Klosterhalfen B, Schumpelick V. Mesh implants in hernia repair. Inflammatory cell response in a rat model. *Eur Surg Res.* 2003; 35:161–6. [PubMed: 12740536]
20. Costello CR, Bachman SL, Grant SA, Cleveland DS, Loy TS, Ramshaw BJ. Characterization of heavyweight and lightweight polypropylene prosthetic mesh explants from a single patient. *Surg Innov.* 2007; 14:168–76. [PubMed: 17928615]
21. Huebner M, Hsu Y, Fenner DE. The use of graft materials in vaginal pelvic floor surgery. *Int J Gynaecol Obstet.* 2006; 92:279–88. [PubMed: 16426613]
22. Mistrangelo E, Mancuso S, Nadalini C, Lijoi D, Costantini S. Rising use of synthetic mesh in transvaginal pelvic reconstructive surgery: a review of the risk of vaginal erosion. *J Minim Invasive Gynecol.* 2007; 14:564–9. [PubMed: 17848316]

23. Kohli N, Walsh PM, Roat TW, Karram MM. Mesh erosion after abdominal sacrocolpopexy. *Obstet Gynecol.* 1998; 92:999–1004. [PubMed: 9840566]
24. Otto J, Kaldenhoff E, Kirschner-Hermanns R, Muhl T, Klinge U. Elongation of textile pelvic floor implants under load is related to complete loss of effective porosity, thereby favoring incorporation in scar plates. *J Biomed Mater Res A.* 2014; 102:1079–84. [PubMed: 23625516]
25. Barone W, Moalli P, Abramowitch S. Variable porosity of common prolapse meshes during uni-axial loading. *Female Pelvic Med Reconstr Surg.* 2013; 19(suppl 2):S56.
26. Majima T, Marchuk LL, Shrive NG, Frank CB, Hart DA. In-vitro cyclic tensile loading of an immobilized and mobilized ligament autograft selectively inhibits mRNA levels for collagenase (MMP-1). *J Orthop Sci.* 2000; 5:503–10. [PubMed: 11180909]
27. Gamble JG, Edwards CC, Max SR. Enzymatic adaptation in ligaments during immobilization. *Am J Sports Med.* 1984; 12:221–8. [PubMed: 6742306]
28. Amiel D, Woo SL, Harwood FL, Akeson WH. The effect of immobilization on collagen turnover in connective tissue: a biochemical-biomechanical correlation. *Acta Orthop Scand.* 1982; 53:325–32. [PubMed: 7090757]
29. Woo SL, Gomez MA, Woo YK, Akeson WH. Mechanical properties of tendons and ligaments. II. The relationships of immobilization and exercise on tissue remodeling. *Biorheology.* 1982; 19:397–408. [PubMed: 7104481]
30. Liu SH, Yang RS, Al-Shaikh R, Lane JM. Collagen in tendon, ligament, and bone healing. A current review. *Clin Orthop Relat Res.* 1995:265–78. [PubMed: 7671527]
31. Eriksen HA, Pajala A, Leppilahti J, Risteli J. Increased content of type III collagen at the rupture site of human Achilles tendon. *J Orthop Res.* 2002; 20:1352–7. [PubMed: 12472252]

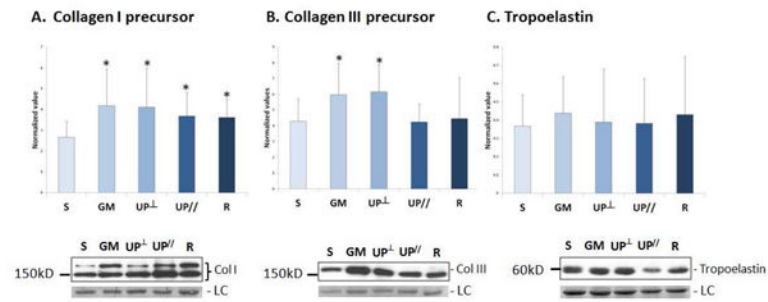


**Figure 1.**

Synthesis of precursors of collagen I and III, and tropoelastin after mesh implantation.

Representative images from Western Blots and bar graphs showing compiled mean (normalized to the values of internal control and loading control) and standard deviation for: A. Collagen I precursor; B. Collagen III precursor; C. Tropoelastin. S = Sham; GM = Gynemesh PS; UP $\perp$  = UltraPro Perpendicular; UP// = UltraPro Parallel; R = Restorelle; LC = loading control. \* indicates significant difference from Sham (P<0.05).

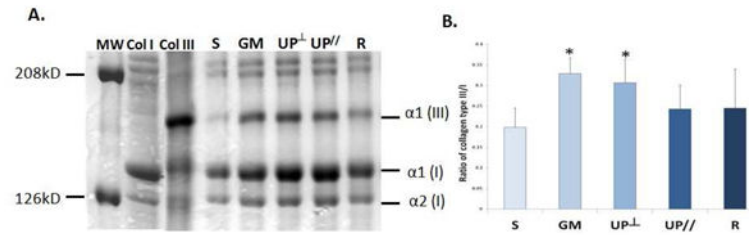


**Figure 2.** Vaginal collagen subtype ratios after mesh implantation. A. Representative SDS-PAGE gel; B. Bar graph showing mean and standard deviation. S = Sham; GM = Gynemesh PS; UP $\perp$  = UltraPro Perpendicular; UP// = UltraPro Parallel; R = Restorelle. \* indicates significant difference from Sham ( $P < 0.05$ ).

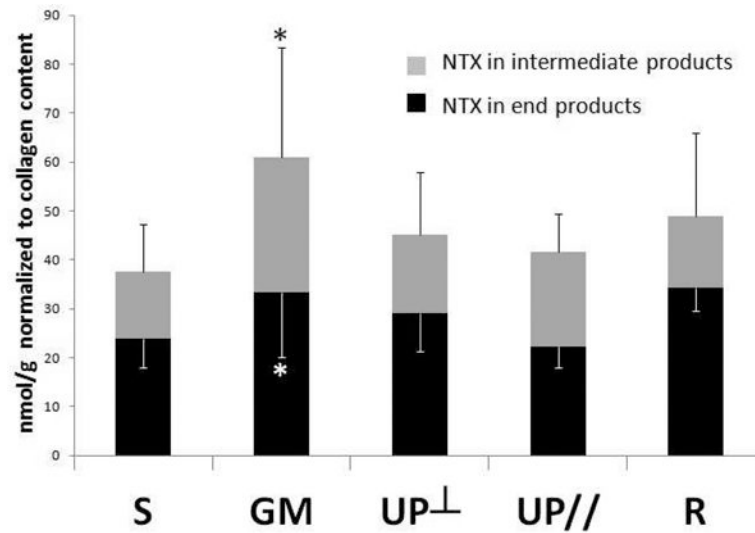


**Figure 3.** Collagen degradation in the vagina after mesh implantation as measured by the amount of N-telopeptidase (NTx) in end degradation products and in intermediate degradation products. S = Sham; GM = Gynemesh PS; UP⊥ = UltraPro Perpendicular; UP// = UltraPro Parallel; R = Restorelle. \* indicates significant difference from Sham (P<0.05).

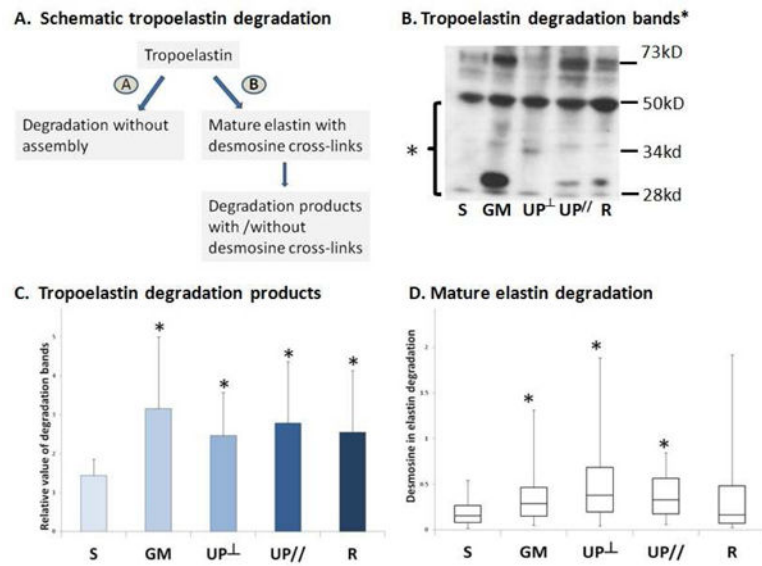


**Figure 4.** Elastin degradation in the vagina after mesh implantation. A. Flow chart elucidates the degradation pathways of elastin; B. Representative western blot image for tropoelastin degradation; C. Bar graph showing the mean and standard deviation of tropoelastin degradation by semi-quantification; D. Box and whisker graph showing the median, first and third quartiles of mature elastin degradation assayed by desmosine crosslink radioimmunoassay. S = Sham; GM = Gynemesh PS; UP<sup>⊥</sup> = UltraPro Perpendicular; UP// = UltraPro Parallel; R = Restorelle. \* indicates significant difference from Sham (P<0.05).



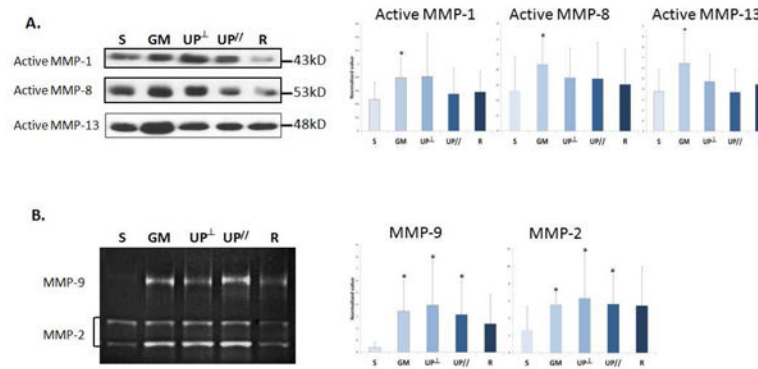


**Figure 5.**

Levels of A. Interstitial collagenase MMPs -1, -8, and -13; B. Elastase MMP-2 and -9 in the vagina after mesh implantation demonstrated by representative images from Western Blots and zymography, and bar graphs showing compiled mean (normalized to the values of internal control and loading control) and standard deviation. S = Sham; GM = Gynemesh PS; UP $\perp$  = UltraPro Perpendicular; UP// = UltraPro Parallel; R = Restorelle. \* indicates significant difference from Sham (P<0.05).

**Table 1**

Demographics of non-human primates in the study. UltraPro Per = UltraPro Perpendicular (low stiffness); UltraPro Par = UltraPro Parallel (high stiffness).

Groups	Age (years) <sup>a</sup>	Parity <sup>b</sup>	Weight (kg) <sup>a</sup>	POPQ Stage <sup>b</sup>
Sham	13.3 ± 2.6	3.5 (2, 6)	7.5 ± 1.3	0 (0, 1)
Gynemesh	12.3 ± 2.4	4 (2, 5)	7.9 ± 1.6	0 (0, 0)
UltraPro Per	12.0 ± 2.5	2 (1.5, 4.5)	7.4 ± 1.3	0 (0, 1)
UltraPro Par	12.9 ± 1.0	4 (4, 5.5)	8.4 ± 1.3	0 (0, 0)
Restorelle	13.8 ± 1.7	5 (3, 5.3)	10.0 ± 2.8	1 (0, 1)
p*	0.43	0.66	0.02	0.30

\* indicates the comparison of overall p value among the groups

<sup>a</sup> indicates mean ± standard deviation

<sup>b</sup> indicates median (1st quartile, 3rd quartile)